LRMP inhibits the cAMP-dependence of HCN4 channels by disrupting intramolecular signal transduction

Colin H Peters[1], Rohit K Singh[2], Avery A Langley[1], William G Nichols[1], Hannah R Ferris[1], Danielle A Jeffrey[1], and Catherine Proenza[1,3,#], John R Bankston[1,#,*]

[1]Department of Physiology and Biophysics, University of Colorado Anschutz Medical Campus, 12800 E. 19th Avenue, Aurora, CO 80045

[2]Skaggs School of Pharmacy, Department of Pharmaceutical Sciences, University of Colorado Anschutz Medical Campus, 12850 E. Montview Boulevard, Aurora, CO 80045

[3]Department of Medicine, Division of Cardiology, University of Colorado Anschutz Medical Campus, 12631 E. 17th Avenue, Aurora, CO 80045

Colin Peters and Rohit Singh contributed equally to this paper

#Equivalent Contribution

*Corresponding Author.

John Bankston, PhD
Department of Physiology & Biophysics
University of Colorado – Anschutz Medical Campus
12800 E. 19th Ave, MS 8307
Aurora, CO 80045
Phone: 303-724-4909
email: john.bankston@cuanschutz.edu

Abstract

Lymphoid restricted membrane protein (LRMP) is a specific regulator of the hyperpolarization-activated cyclic nucleotide-sensitive isoform 4 (HCN4) channel. LRMP prevents cAMP-dependent potentiation in HCN4 but the interaction domains, mechanisms of action, and basis for isoform-specificity remain unknown. Here we identify the domains of LRMP essential for regulation, we show that LRMP acts by disrupting the intramolecular signal transduction between cyclic nucleotide binding and gating, and we demonstrate that non-conserved regions in HCN4 are required for LRMP isoform-specificity. Using patch clamp electrophysiology and Förster resonance energy transfer (FRET), we show that the initial 227 residues of LRMP and the N-terminus of HCN4 are necessary for LRMP to interact with HCN4. We also found that the HCN4 N-terminus and HCN4-specific residues in the C-linker are necessary for regulation of HCN4 by LRMP. Taken together, these results suggest that LRMP modulates HCN4 through an isoform-specific interaction involving the N-terminals of both proteins, and that this interaction inhibits the transduction between cAMP binding and channel activation via an interface involving the N-terminus, C-linker, and S4-S5 linker of HCN4.

Introduction

Hyperpolarization-activated, cyclic nucleotide-sensitive (HCN) ion channels are biophysical anomalies. Despite being structurally related to voltage-gated K^+ channels, they activate in response to membrane hyperpolarization and pass a mixed Na^+/K^+ current. In addition, binding of cyclic nucleotides, particularly cAMP, to a conserved C-terminal cyclic nucleotide binding domain (CNBD) potentiates HCN channels by shifting the voltage-dependence of activation to more depolarized potentials, speeding activation, and slowing deactivation (DiFrancesco and Tortora, 1991; Wainger et al., 2001).

While the details of intramolecular transduction between cAMP binding and channel gating are yet to be fully elucidated, some key aspects are known: 1) the unbound CNBD is inhibitory — truncation of the CNBD potentiates the channel activation, similar to cAMP binding to the intact CNBD (Wainger et al., 2001); 2) the slowing of channel deactivation in response to cAMP binding occurs through a separate mechanism from the shift in activation voltage dependence, and cannot be replicated by truncation of the CNBD (Wicks et al., 2011; Sunkara et al., 2018); and 3) transduction of the signal for the cAMP-dependent shift in channel activation, but not deactivation, requires interactions between the C-linker, the N-terminal HCN domain (HCND), and the S4-S5 linker (Porro et al., 2019; Wang et al., 2020b).

Several proteins interact with HCN channels to modulate their activity (Peters et al., 2022). The inositol 1,4,5-triphosphate receptor-associated proteins, IRAG1 and LRMP/IRAG2 (lymphoid restricted membrane protein), are a family of endoplasmic reticulum (ER) transmembrane proteins that are isoform-specific regulators of HCN4 (Peters et al., 2020). IRAG and LRMP share some sequence homology, particularly in their coiled-coil motifs, and both have been found to regulate IP_3 receptor calcium release (Schlossmann et al., 2000;

Geiselhöringer et al., 2004; Prüschenk et al., 2021). However, LRMP and IRAG have opposing effects on HCN4: IRAG1 causes a gain-of-function by shifting HCN4 activation to more depolarized membrane potentials in the absence of cAMP; in contrast, LRMP causes loss-of-function by inhibiting cAMP-dependent potentiation of HCN4 activation (Peters et al., 2020).

In this study, we focused on LRMP and investigated the interaction domains and mechanism by which it inhibits cAMP-dependent shifts in HCN4 activation. Our previous study showed that LRMP differs considerably from TRIP8b, a neuronal protein that also prevents cAMP-dependent shifts in HCN channel activation through direct antagonism of cAMP binding (Santoro et al., 2004; Zolles et al., 2009; Bankston et al., 2017; Saponaro et al., 2018). LRMP doesn't appear to inhibit cAMP binding to the CNBD, as cAMP retains the ability to slow channel deactivation in the presence of LRMP (Peters et al., 2020). Furthermore, TRIP8b regulates all HCN channel isoforms (Zolles et al., 2009; Santoro et al., 2011), whereas LRMP is specific for the HCN4 isoform (Peters et al., 2020). These observations suggest that LRMP regulates HCN4 by interfering with an isoform-specific step in the signal transduction pathway that links cAMP binding to the shift in activation voltage dependence.

We tested this hypothesis using a combination of patch clamp electrophysiology and FRET. We found that the initial N-terminal 227 residues of LRMP bind to the N-terminus of HCN4 and that the intact HCN4 N-terminus is required for channel regulation by LRMP. Furthermore, we show that two HCN4-specific residues in the C-linker, P545 and T547, are necessary for LRMP to inhibit channel activation, consistent with a model in which LRMP acts via a signal transduction centre formed by the C-linker, N-terminus, and S4-S5 linker.

Materials and Methods

DNA Constructs

The LRMP construct in PCMV6-Kan/Neo, HCN1 in pcDNA3 (generously provided by Dr. Eric Accili), HCN4-2 in pcDNA3.1, HCN4-S719X in pCDNA3.1, and HCN4 Δ1-25 in pcDNA6 (also known as HCN4s, generously provided by Dr. Richard Aldrich) have been described previously (Proenza et al., 2002; Liao et al., 2012; Liu and Aldrich, 2011; Peters et al., 2020). HCN2 was subcloned from pcDNA4 into pcDNA3.1 for this study. Other constructs were synthesized by Twist Biosciences or using site-directed mutagenesis either in-house or by Applied Biological Materials. The HCN4 Δ1-65, HCN4 Δ1-130, and HCN4 Δ1-185 deletion clones were made using a site-directed mutagenesis kit (New England Biolabs) and a codon-optimized HCN4 plasmid in the pTwist-CMV-WPRE-Neo vector synthesized by Twist Biosciences. For FRET experiments, recombinant fusions of mHCN4 and mLRMP were constructed by introducing Cerulean (CER) or Citrine (CIT) fluorescent proteins using PCR-based cloning. The C-termini of HCN4 constructs were tagged with CER, while the C-termini of LRMP constructs were tagged with CIT. All clones used in this study are the murine sequences. All new constructs were confirmed by DNA sequencing (Barbara Davis Center BioResource Core, ACGT, or Plasmidsaurus). Detailed information about constructs can be found in supplemental table S1.

Cell Lines

HEK 293 cells (ATCC) were grown in a humidified incubator at 37°C and 5% CO_2 in high glucose DMEM with L-glutamine supplemented with 10% FBS, 100 U/mL penicillin, and 100 µg/mL streptomycin. Cells were transfected 48 hours prior to experiments and were plated

on either protamine-coated glass coverslips (for patch clamp experiments) or poly-d-lysine coated glass-bottom dishes (for FRET experiments).

Patch clamp experiments were performed in either transiently transfected HEK293 cells, an HCN4 stable line in HEK293 cells (Zong et al., 2012), or seven new stable cell lines in HEK293 cells: HCN2, HCN4 Δ1-65, HCN4 Δ1-130, HCN4 Δ1-185, HCN4 Δ1-200, HCN2 A467P/F469T (HCN2 AF/PT), and HCN4 P545A/T547F (HCN4 PT/AF). Stable cell lines were made by transfecting HEK293 cells with the respective plasmids using Lipofectamine 2000 (Invitrogen) according to the manufacturer's instructions. 48 hours post-transfection, 200 ug/mL of G418 disulfate (Alfa Aesar) was added to the cell culture media in place of pen-strep to select for stably transfected cells. Single cell clones were tested using whole-cell patch clamp and the clonal lines that exhibited the largest and most consistent currents were grown into stable cell lines.

Transient transfection of HCN4 constructs and/or LRMP was performed using Fugene6 (Promega) according to the manufacturer's instructions. Transfections of all constructs that did not include fluorescent tags were performed with the addition of eGFP as a co-transfection marker.

Patch Clamp Electrophysiology

Cells were plated on sterile protamine-coated glass coverslips 24-48 hours prior to experiments. Cells on coverslip shards were transferred to the recording chamber and perfused (~0.5 to 1 mL/min) with extracellular solution containing (in mM): 30 KCl, 115 NaCl, 1 $MgCl_2$, 1.8 $CaCl_2$, 5.5 glucose, and 5 HEPES. Transiently transfected cells were identified by green fluorescence.

Patch pipettes were pulled from borosilicate glass to a resistance of 1.0-3.0 MOhm when filled with intracellular solution containing (in mM): 130 K-Aspartate, 10 NaCl, 1 EGTA, 0.5 $MgCl_2$, 5 HEPES, and 2 Mg-ATP. 1 mM cAMP was added to the intracellular solution as indicated. All recordings were performed at room temperature in the whole-cell configuration. Data were acquired at 5 KHz, and low-pass filtered at 10 KHz using an Axopatch 200B amplifier (Axon Instruments), Digidata 1440A A/D converter and Clampex software (Molecular Devices). Pipette capacitance was compensated in all recordings. Membrane capacitance and series resistance (Rs) were estimated in whole-cell experiments using 5-mV test pulses. Only cells with Rs <10 MOhm were analyzed. Data were analyzed in Clampfit 10.7 (Molecular Devices).

Channel activation was determined from peak tail current amplitudes at -50 mV following 3-s hyperpolarizing pulses to membrane potentials between -50 mV and -170 mV from a holding potential of 0 mV. Normalized tail current-voltage relationships were fit by single Boltzmann equations to yield values for the midpoint activation voltage ($V_{1/2}$) and slope factor (k). All reported voltages are corrected for a calculated +14 mV liquid junction potential between the extracellular and intracellular solutions.

FRET Hybridization Assays

HEK293 cells expressing HCN4-CER and LRMP-CIT fusion proteins were examined 48 h after transfection using a Zeiss LSM 710 confocal laser scanning microscope. An area of 500–2,500 μm^2 was selected from the overall field of view. Images were taken through a 40× water objective. CER and CIT were excited with separate sweeps of the 458- and 514-nm laser lines of an argon laser directed at the cell with a 458/514-nm dual dichroic mirror. Relative to full power, the excitation power for the imaging sweeps was attenuated to 1% for CER and 0.5% for Citrine.

Bleaching was performed by using multiple (20–60) sweeps of the CIT laser at full power. Bleaching was usually complete within 1-2 m. Emitted light was collected between 449 and 488 nm for CER and 525 and 600 nm for CIT. With this setup, there was no contamination of the relevant CER signal from the CIT. For each experiment, the photomultiplier tube gain was adjusted to ensure that the maximum pixel intensity was not >70% saturated. Fluorescence intensity was then measured by drawing regions of interest (ROIs) around the cytoplasmic portion of the cell in ImageJ (Schneider et al., 2012). Masks were occasionally used to eliminate bright fluorescent puncta within the cell (this was a rare occurrence in the CER signal). Percent FRET (E) was calculated as:

$$E= [I_{CERpost} - I_{CERpre}]/ I_{CERpost} * 100,$$

where $I_{CERpost}$ is the CER intensity after bleaching and I_{CERpre} is the CER intensity before bleaching.

Statistical Analysis

All statistical analysis was performed using JMP 15 software (SAS Institute). Tests for differences in the average midpoint of activation for a given HCN channel construct in the presence of LRMP and/or 1 mM cAMP were performed with a 2-way ANOVA. The main independent variables were the absence or presence of LRMP and the absence or presence of 1 mM cAMP in the pipette solution. Differences in the effects of cAMP in the absence or presence of LRMP were analyzed using an interaction term between the main independent variables. $P < 0.05$ was used as the cut-off for a significant effect in all cases.

Results

The N-terminus of LRMP is necessary and sufficient to regulate HCN4

We previously showed that LRMP significantly reduces the cAMP-dependent depolarizing shift in HCN4 activation and that it does not regulate HCN1 or HCN2 (Peters et al., 2020). We next sought to identify a subdomain within LRMP that is responsible for this regulation. We began with a truncated LRMP construct with a citrine fluorescent protein replacing the C-terminal ER transmembrane and lumenal domains (LRMP 1-479Cit; **Figs. 1A** and **1B**; **Table 1**). We found that LRMP 1-479Cit inhibited HCN4 to an even greater degree than the full-length LRMP, likely because expression of this tagged construct was improved compared to the untagged full-length LRMP, which was detected by co-transfection with GFP. A key feature of LRMP in our original study is that it does not prevent binding of cAMP to the CNBD of HCN4. This was also the case for LRMP 1-479Cit, as indicated by the significant slowing of deactivation by cAMP even in the presence of LRMP 1-479Cit ($P = 0.0036$; **Fig. 1C**). These results indicate that the ER transmembrane and luminal domains of LRMP are not required for regulation of HCN4 and they support the idea that LRMP limits cAMP potentiation of HCN4 by interfering with a downstream step in the cAMP signal transduction pathway.

To further resolve which regions of LRMP are required to regulate HCN4, we tested a series of additional truncated LRMP constructs (**Fig. 2**) for their ability to prevent cAMP-dependent shifts in HCN4 activation. We first split LRMP into two fragments: the LRMP 1-227 construct contains the N-terminus of LRMP with a cut-site near the N-terminus of the predicted coiled-coil sequence, while LRMP 228-539 contains the remainder of the protein. We found that LRMP 1-227 recapitulated the effects of full-length LRMP, while LRMP 228-539 had no effect on HCN4 gating (**Figs. 2A**, **2B**, and **2E**; **Table 2**). However, when we further split the N-

terminal domain of LRMP into two fragments, neither LRMP 1-108 nor LRMP 110-230 regulated HCN4 (**Figs. 2C**, **D**, and **2E**; **Table 2**). Thus, the first 227 residues of LRMP are sufficient to regulate HCN4, with residues in both halves of the LRMP N-terminus necessary for the regulation.

The N-terminus of HCN4 is required for regulation by LRMP

We next examined the domains of the HCN4 channel that are necessary for regulation by LRMP. Since LRMP regulates only the HCN4 isoform, we focused on the large non-conserved regions in the distal N- and C-terminals as potential sites for LRMP regulation. We first examined the N-terminus by testing the ability of LRMP to regulate a series of HCN4 channels with progressively larger truncations (Δ1-25, Δ1-65, Δ1-130, Δ1-185, and Δ1-200). The four smaller deletions all produced functional channels with normal cAMP-dependent shifts in activation (**Fig. 3**), while the HCN4 Δ1-200 construct produced insufficient current amplitude for analysis.

When the first 25 residues in the HCN4 N-terminus were truncated, LRMP still prevented cAMP from shifting HCN4 activation, just as in the WT HCN4 channel **(Fig. 3A** and **3E**; **Table 1**). Truncation of residues 1-62 led to a partial LRMP effect where cAMP caused a significant depolarizing shift in the presence of LRMP, but the activation in the presence of LRMP and cAMP was hyperpolarized compared to cAMP alone (**Fig. 3B, C** and **3E**; **Table 1**). In the HCN4Δ1-130 construct, cAMP caused a significant depolarizing shift in the presence of LRMP; however, the midpoint of activation in the presence of LRMP and cAMP showed a non-significant trend towards hyperpolarization compared to cAMP alone (**Fig. 3C** and **3E**; **Table 1**). Finally, truncation of the first 185 residues, which removes most of the non-conserved region of

the HCN4 N-terminus, completely abolished LRMP regulation of the channel (**Fig. 3D** and **3E**; **Table 1**); when LRMP was present cAMP caused a significant depolarizing shift in the HCN4 Δ1-185 activation, and the midpoint of activation in the presence of both LRMP and cAMP was not significantly different from the midpoint in the presence of cAMP alone. These results suggest that the non-conserved region in the N-terminus of HCN4 are a primary site for functional regulation by LRMP.

We also investigated LRMP regulation of two C-terminal truncations in HCN4: HCN4 S719X, which removes the C-terminus distal to the CNBD (Liao et al., 2012), and HCN4 V604X, which additionally removes the CNBD. Truncation of the distal C-terminus did not prevent LRMP regulation. In the presence of both LRMP and cAMP the activation of HCN4-S719X was still significantly hyperpolarized compared to the presence of cAMP alone (**Figs. 4A** and **4B**; **Table 1**). And the cAMP-induced shift in HCN4-S719X in the presence of LRMP (~7 mV) was less than half the shift in the absence of LRMP (~18 mV). HCN4-V604X, which truncates the channel between the C-linker and CNBD, shifts channel activation to more depolarized potentials and prevents cAMP-dependent regulation (**Figs. 4C** and **4D**; **Table 1**). This is similar to the effects of the homologous HCN2-V526X mutant (Wainger et al., 2001). LRMP did not alter the gating of HCN4-V604X in the absence of cAMP, and the lack of cAMP binding limits the investigation of any LRMP inhibition of cAMP-dependent potentiation (**Figs. 4C** and **4D**). Together, these results show significant LRMP regulation of HCN4 even when the distal C-terminus is truncated, consistent with a minimal role for the C-terminus in the regulatory pathway.

The N-terminus of LRMP associates with the N-terminus of HCN4

We next used FRET hybridization assays to examine potential interactions between small fragments of LRMP and HCN4 in a cellular environment. This approach has been used to define interactions between the N- and C-termini of EAG channels as well as between Calmodulin and $Ca_V1.2$ (Gianulis et al., 2013; Erickson et al., 2003). Fragments of LRMP tagged on the C-terminus with Citrine and fragments of HCN4 tagged on the C-terminus with Cerulean were co-expressed in HEK293 cells and FRET was assessed using the acceptor photobleaching method (**Fig. 5**; **Table 3**) (Bastiaens and Jovin, 1996; Wouters et al., 1998; Klipp et al., 2020).

A Citrine-tagged construct corresponding to the functionally active domain of LRMP (LRMP 1-230) did not significantly FRET with the full-length HCN4 N-terminus (HCN4 NF, residues1-260; **Fig. 5A**). However, these fragments are large and may orient the fluorophores at a distance outside of the range for FRET, which is ~20-80Å. Indeed, when we expressed LRMP 1-230 with smaller fragments of the HCN4 N-terminus — HCN4 N1 (residues 1-125) and HCN4 N2 (residues 126-260) — we measured significant FRET compared to control cells co-transfected with Cer-HCN4 fragments and Citrine alone (i.e., without any LRMP sequence; **Fig. 5A**). Smaller fragments of LRMP — LRMP L1 (residues1-108) and LRMP L2 (residues 110-230) also exhibited significant FRET with the whole HCN4 N-terminus and with HCN4 N-terminal fragments (**Fig. 5B**). No significant FRET was observed between LRMP fragments and the HCN2 N-terminus, which shares the conserved HCND with HCN4 (**Figs. 5B**). None of the LRMP fragments tested exhibited significant FRET with the HCN4 CNBD compared to control experiments (**Fig. 3A** and **3B**; **Table 3**). Ultimately these data suggest that LRMP interacts with the non-conserved distal N-terminus of HCN4.

Mutants in the HCN4 C-linker disrupt LRMP's functional effects

Prior work has shown that transduction of cAMP-binding to shifts in channel activation require a tripartite interaction of the N-terminal HCND, the C-linker, and the S4-S5 linker (Porro et al., 2019; Wang et al., 2020b; Kondapuram et al., 2022). Since LRMP interacts with the HCN4 N-terminus and disrupts cAMP-dependent potentiation downstream of the cAMP binding site, we hypothesized that it may act via this cAMP transduction centre. Although most elements of the transduction centre are conserved among HCN channel isoforms, the C-linker conformation differs subtly between structures of HCN1 and HCN4 (**Fig. 6A**; Lee and MacKinnon, 2017; Saponaro et al., 2021). We identified two HCN4-specific residues, P545 and T547 in the C-linker, that are close in proximity to the transduction centre that could account for these changes (**Fig. 6A**). When we mutated these residues to the analogous HCN2 amino acids, the HCN4-P545A/T547F channel responded normally to cAMP with an ~10 mV shift in activation voltage (**Figs. 6B** and **6C**; **Table 1**). However, HCN4-P545A/T547F was insensitive to LRMP (**Figs. 6B** and **6C**; **Table 1**), indicating that the unique HCN4 C-linker is necessary for regulation by LRMP. The HCN4 C-linker alone was not sufficient to confer regulation by LRMP onto HCN2 in the reverse mutant (HCN2 A467P/F469T), consistent with our data showing that the HCN4 N-terminus is also required (**Figs. 6D** and **6E**; **Table 1**). Thus, LRMP appears to regulate HCN4 by altering the interactions between the C-linker, S4-S5 linker, and N-terminus at the cAMP transduction centre.

The HCN4 N-Terminus and cAMP transduction centre confer LRMP regulation to HCN2

Given that LRMP requires the unique HCN4 N-terminus to regulate the channel, we investigated whether this region is sufficient to confer LRMP regulation to HCN2 channels,

which are normally LRMP-insensitive. We found that a previously described HCN4-2 chimera containing the HCN4 N-terminus and transmembrane domains (residues 1-518) with the HCN2 C-terminus (442-863) (Liao et al., 2012) was partially regulated by LRMP (**Fig. 7A** and **7B**). In the presence of LRMP and 1 mM cAMP, the HCN4-2 activation was shifted towards more hyperpolarized potentials compared to the presence of 1 mM cAMP alone and the magnitude of the cAMP-dependent shift in activation was reduced from ~20 mV in the absence of LRMP to ~9 mV when LRMP was present. Because this construct still contains the HCN2 C-linker sequence, we next made a targeted chimera of HCN2 that contains the distal HCN4 N-terminus (residues 1-212) and the HCN2 transmembrane and C-terminal domains with 5 point mutants in non-conserved residues of the S5 segment and C-linker elbow (M338V/C341V/S345G/A467P/F469T). The resulting HCN4-2 VVGPT channel has a similar voltage-dependence of activation as HCN2 and a normal response to cAMP in the absence of LRMP (**Table 1**; **Fig. 7C** and **7D**). Importantly, the HCN4-2 VVGPT channel is insensitive to cAMP in the presence of LRMP (**Fig. 7C** and **7D**), indicating that the HCN4 N-terminus and cAMP-transduction centre residues are sufficient to confer LRMP regulation to HCN2.

Discussion

LRMP is one of only two isoform-specific regulators of HCN4 to be discovered. Importantly, this study of LRMP's mechanisms of action also reveals unique features of HCN4 function that could contribute to its physiological roles and could inform development of isoform-specific drugs. Although LRMP prevents cAMP-dependent shifts in HCN4 activation, it does not act by preventing cAMP from binding to the channel. Instead, we show here that the N-terminal domains of LRMP and HCN4 are required for both physical interaction and regulation.

Our data further show that LRMP acts by disrupting transduction between cAMP binding and the shift in voltage-dependence in a manner that depends on HCN4-specific residues in the C-linker that are in close proximity to a previously described cAMP transduction centre formed by the C-linker, N-terminus, and S4-S5 linker.

An intramolecular transduction centre between the C-Linker, HCND, and S4-S5 linker links cAMP binding to shifts in activation.

The binding of cAMP to the CNBD of HCN channels causes two distinct effects – a depolarizing shift in the voltage-dependence of activation and a slowing of channel deactivation (Wicks et al., 2011; Sunkara et al., 2018). The slowed deactivation appears to be caused by stabilization of the open state in the presence of cAMP (Wicks et al., 2009, 2011; Hummert et al., 2018). In contrast, voltage-clamp fluorimetry experiments and computational modelling suggest that shifts in channel activation are caused by a hyperpolarized voltage-dependence of S4 movement in the presence of cAMP (Magee, 2017; Hummert et al., 2018). The two separate cAMP effects allows slowing of deactivation to be used as a proxy for cAMP binding even in the absence of cAMP-dependent shifts in activation (Liao et al., 2012; Porro et al., 2019; Peters et al., 2020).

Recent studies indicate that the cAMP-dependent shift in activation requires an intramolecular cAMP transduction centre formed by interactions between the C-linker, N-terminal HCND, and S4-S5 linker (Weißgraeber et al., 2017; Porro et al., 2019; Wang et al., 2020b; Saponaro et al., 2021; Kondapuram et al., 2022). The inhibitory effects of the unbound CNBD are stabilized by an interaction between a conserved lysine in the C-linker elbow (K542 in HCN4; **Fig. 8A**) with the HCND of the adjacent subunit at M233 (Porro et al., 2019;

Kondapuram et al., 2022), likely through a downstream hydrophobic contact between the HCND and the voltage sensor (Porro et al., 2019; Elbahnsi et al., 2023). Another interaction, between the C-linker residue E556 and R232 on the HCND of the same subunit, is required for the cAMP-dependent shift in activation (Porro et al., 2019; Wang et al., 2020b). The K542A/E556A double mutation eliminates the cAMP-dependent shift in activation, but not the slowing of deactivation (Porro et al., 2019). Interestingly, the S4-S5 linker does not appear to be required for voltage-dependent gating in HCN channels (Flynn and Zagotta, 2018; Cowgill et al., 2019). However, in HCN4 a Mg^{2+} coordination site between residues H406 and D410 on the S4-S5 linker and H552 and E566 on the C-linker is required for the cAMP-dependent shift in activation (**Fig 6A**; **Fig. 8A**; Saponaro et al., 2021).

Proposed model: LRMP disrupts cAMP regulation of HCN4 activation at the cAMP transduction centre.

In our proposed model for how LRMP disrupts the cAMP-dependent shift in HCN4 activation (**Fig. 8**), LRMP is bound to HCN4 through an interaction between the distal N-terminus of HCN4 and the N-terminus of LRMP. Within the HCN4 N-terminus, the HCND, which is conserved across isoforms, is known to be required for functional channel expression (Tran et al., 2002; Wang et al., 2020b). However, little is known about the function of the more distal HCN4 N-terminus, which is not resolved in channel structures (Lee and MacKinnon, 2017; Saponaro et al., 2021) and not conserved between HCN channel isoforms. We found that truncation of the non-conserved HCN4 N-terminus abolishes regulation by LRMP without affecting other aspects of HCN4 function. This finding was further corroborated by FRET

experiments showing interactions between LRMP and the HCN4 N-terminus, but not the CNBD or more distal C-terminal regions.

We hypothesize that the interaction with the N-terminus of HCN4 allows LRMP to allosterically disrupt the transduction between cAMP binding and channel activation. Unlike the neuronal protein TRIP8b, which directly competes for the cAMP binding site to regulate all HCN channel isoforms (Bankston et al., 2017; Saponaro et al., 2018), LRMP doesn't appear to act at the cAMP binding site, as cAMP still slows deactivation in the presence of LRMP (**Fig. 1C**). In support of this model, we did not measure significant FRET between Citrine-tagged LRMP fragments and the Cerulean-tagged CNBD (**Fig. 5**). Because of the known interactions of the C-linker with the N-terminal HCND (Porro et al., 2019; Wang et al., 2020b; Kondapuram et al., 2022), we looked for unique residues in the HCN4 C-linker that could be necessary for functional regulation by LRMP. Interestingly, two C-linker residues, P545 and T547, between the sites of interaction with the HCND are conserved in HCN4 across mammalian species, but are not conserved in HCN1 or HCN2 (**Fig. 6A**). Given that these residues are the only ones in the region that differ between isoforms, they appear to be responsible for the different orientations of the C-linker in the HCN1 and HCN4 cryoEM structures (Lee and MacKinnon, 2017; Saponaro et al., 2021).

Despite their homology, cAMP signal transduction in HCN4 appears less robust than in HCN2. The cAMP-dependent shift in HCN4 (~14 mV) is smaller than in HCN2 (~20 mV; **Table 1**); in HCN4, but not HCN2, the transduction of cAMP is sensitive to divalent cations (Saponaro et al., 2021; Peters et al., 2023); and cAMP-dependent shifts in activation can be disrupted in HCN4 by regulatory factors such as cyclic-dinucleotides and LRMP (Lolicato et al., 2014), It's likely that the difference in orientation of the C-linker relative to the S4-S5 linker accounts for

differences in cAMP signal transduction in HCN4 compared to HCN2. Indeed, mutating the non-conserved residues to the corresponding HCN2 amino acids (P545A/T547F) abolishes LRMP regulation of HCN4 (**Fig. 6**). Importantly, chimeric HCN2 channels that include the distal HCN4 N-terminus as well as mutations in non-conserved residues in S5 and the C-linker are rendered LRMP sensitive (**Fig. 7**). These experiments not only show that LRMP acts via this region, but also suggest that the orientation of the C-linker elbow is critical for isoform-specific regulation in HCN4.

Potential physiological implications

The first half of LRMP's cytosolic domain (residues 1-230) that make up the N-terminus of the protein is necessary and sufficient to interact with and regulate HCN4. Because the C-terminus of LRMP is embedded in the ER, the N-terminal region of LRMP would naturally be in closer proximity to HCN4 in the plasma membrane. LRMP also interacts with and regulates Ca^{2+} release through inositol triphosphate (IP_3) receptors in the ER membrane, likely via a site in the coiled-coil region (Prüschenk et al., 2021). Together these results suggest the intriguing possibility of coordination between the activity of IP_3Rs and HCN4 and the formation of ER-plasma membrane junctions in cells where LRMP and HCN4 are co-expressed. For example, in sinoatrial myocytes HCN4 and SR Ca^{2+} release, including through IP3 receptors, are both known to regulate pacemaking (DiFrancesco, 2010; Peters et al., 2021; Capel et al., 2021). A potential interaction with LRMP (or IRAG1), could serve to coordinate these important processes. Thus, future studies to identify tissues where LRMP and HCN4 are co-expressed are of clear importance.

Limitations

Unfortunately, the available HCN4 structures do not resolve the distal N-terminus (Shintre* et al., 2018; Saponaro et al., 2021), and the structure of LRMP has yet to be resolved. This lack of structural information hindered our decisions about specific cut sites for LRMP and HCN4 constructs and restricts our ability to predict the precise residues that are involved in the described interactions. For example, we found that LRMP interacts with isolated fragments representing each half of the HCN4 N-terminus. This could be explained by a diffuse interaction, multiple sites, or our cut site overlapped the interaction site. The partial disruption of LRMP's functional regulation in the HCN4 Δ1-62 and Δ1-130 deletions suggest that multiple or diffuse interactions are more likely, but we are unable to give a definitive conclusion. Ultimately, these questions will require a structure the LRMP-HCN4 interaction sites.

Summary

Overall, these data support a model for LRMP regulation of HCN4 where LRMP interacts with the HCN4 N-terminus (**Fig. 8**) to allosterically disrupt cAMP signal transduction between the C-linker, N-terminus, and S4-S5 linker (Porro et al., 2019; Wang et al., 2020b). Our data suggest that LRMP disrupts the C-linker from transferring the cAMP-dependent conformational change in the CNBD to this transduction-centre, thereby preventing activation potentiation. The isoform specificity is determined by both the unique distal N-terminus and the unique orientation of the C-linker of HCN4. While a potential physiological role for LRMP regulation of HCN4 remains unknown, our data show that LRMP is a useful biophysical tool to study the intramolecular signal transduction between cAMP binding and the shift in HCN4 activation.

Acknowledgements

This work was funded by NIH grants R01HL088427 and R01GM140004 to CP and R35GM137912 to JB. CHP was funded by an American Heart Association Postdoctoral Fellowship 830889. The authors gratefully acknowledge the contributions of Abby Camenisch and Karin Nunley.

The authors declare they have no conflict of interest.

References

Bankston, J.R., H.A. DeBerg, S. Stoll, and W.N. Zagotta. 2017. Mechanism for the inhibition of the cAMP dependence of HCN ion channels by the auxiliary subunit TRIP8b. *J. Biol. Chem.* jbc.M117.800722. doi:10.1074/jbc.M117.800722.

Bastiaens, P.I., and T.M. Jovin. 1996. Microspectroscopic imaging tracks the intracellular processing of a signal transduction protein: fluorescent-labeled protein kinase C beta I. *Proc Natl Acad Sci U S A*. 93:8407–8412. doi:10.1073/pnas.93.16.8407.

Capel, R.A., S.J. Bose, T.P. Collins, S. Rajasundaram, T. Ayagama, M. Zaccolo, R.-A.B. Burton, and D.A. Terrar. 2021. IP3-mediated Ca2+ release regulates atrial Ca2+ transients and pacemaker function by stimulation of adenylyl cyclases. *Am J Physiol Heart Circ Physiol*. 320:H95–H107. doi:10.1152/ajpheart.00380.2020.

Cowgill, J., V.A. Klenchin, C. Alvarez-Baron, D. Tewari, A. Blair, and B. Chanda. 2019. Bipolar switching by HCN voltage sensor underlies hyperpolarization activation. *Proc Natl Acad Sci U S A*. 116:670–678. doi:10.1073/pnas.1816724116.

DiFrancesco, D. 2010. The role of the funny current in pacemaker activity. *Circ Res*. 106:434–446. doi:10.1161/CIRCRESAHA.109.208041.

DiFrancesco, D., and P. Tortora. 1991. Direct activation of cardiac pacemaker channels by intracellular cyclic AMP. *Nature*. 351:145–147. doi:10.1038/351145a0.

Elbahnsi, A., J. Cowgill, V. Burtscher, L. Wedemann, L. Zeckey, B. Chanda, and L. Delemotte. 2023. Interplay between VSD, pore, and membrane lipids in electromechanical coupling in HCN channels. *Elife*. 12:e80303. doi:10.7554/eLife.80303.

Erickson, M.G., H. Liang, M.X. Mori, and D.T. Yue. 2003. FRET two-hybrid mapping reveals function and location of L-type Ca2+ channel CaM preassociation. *Neuron*. 39:97–107. doi:10.1016/s0896-6273(03)00395-7.

Flynn, G.E., and W.N. Zagotta. 2018. Insights into the molecular mechanism for hyperpolarization-dependent activation of HCN channels. *Proc. Natl. Acad. Sci. U.S.A.* 115:E8086–E8095. doi:10.1073/pnas.1805596115.

Geiselhöringer, A., M. Werner, K. Sigl, P. Smital, R. Wörner, L. Acheo, J. Stieber, P. Weinmeister, R. Feil, S. Feil, J. Wegener, F. Hofmann, and J. Schlossmann. 2004. IRAG is essential for relaxation of receptor-triggered smooth muscle contraction by cGMP kinase. *EMBO J.* 23:4222–4231. doi:10.1038/sj.emboj.7600440.

Gianulis, E.C., Q. Liu, and M.C. Trudeau. 2013. Direct interaction of eag domains and cyclic nucleotide-binding homology domains regulate deactivation gating in hERG channels. *J Gen Physiol*. 142:351–366. doi:10.1085/jgp.201310995.

Hummert, S., S. Thon, T. Eick, R. Schmauder, E. Schulz, and K. Benndorf. 2018. Activation gating in HCN2 channels. *PLOS Computational Biology*. 14:e1006045. doi:10.1371/journal.pcbi.1006045.

Klipp, R.C., M.M. Cullinan, and J.R. Bankston. 2020. Insights into the molecular mechanisms underlying the inhibition of acid-sensing ion channel 3 gating by stomatin. *J Gen Physiol*. 152:e201912471. doi:10.1085/jgp.201912471.

Kondapuram, M., B. Frieg, S. Yüksel, T. Schwabe, C. Sattler, M. Lelle, A. Schweinitz, R. Schmauder, K. Benndorf, H. Gohlke, and J. Kusch. 2022. Functional and structural characterization of interactions between opposite subunits in HCN pacemaker channels. *Commun Biol*. 5:430. doi:10.1038/s42003-022-03360-6.

Lee, C.-H., and R. MacKinnon. 2017. Structures of the Human HCN1 Hyperpolarization-Activated Channel. *Cell*. 168:111-120.e11. doi:10.1016/j.cell.2016.12.023.

Liao, Z., D. Lockhead, J.R. St Clair, E.D. Larson, C.E. Wilson, and C. Proenza. 2012. Cellular context and multiple channel domains determine cAMP sensitivity of HCN4 channels: ligand-independent relief of autoinhibition in HCN4. *J Gen Physiol*. 140:557–566. doi:10.1085/jgp.201210858.

Liu, H., and R.W. Aldrich. 2011. Tissue-specific N terminus of the HCN4 channel affects channel activation. *J. Biol. Chem.* 286:14209–14214. doi:10.1074/jbc.M110.215640.

Lolicato, M., A. Bucchi, C. Arrigoni, S. Zucca, M. Nardini, I. Schroeder, K. Simmons, M. Aquila, D. DiFrancesco, M. Bolognesi, F. Schwede, D. Kashin, C.W.G. Fishwick, A.P. Johnson, G. Thiel, and A. Moroni. 2014. Cyclic dinucleotides bind the C-linker of HCN4 to control channel cAMP responsiveness. *Nat Chem Biol*. 10:457–462. doi:10.1038/nchembio.1521.

Magee, K.E.A. 2017. HCN channel gating models: a re-evaluation based on how the voltage-sensing and cAMP-sensing domains regulate kinetics.

Peters, C.H., P.W. Liu, S. Morotti, S.C. Gantz, E. Grandi, B.P. Bean, and C. Proenza. 2021. Bidirectional flow of the funny current (If) during the pacemaking cycle in murine sinoatrial node myocytes. *PNAS*. 118. doi:10.1073/pnas.2104668118.

Peters, C.H., M.E. Myers, J. Juchno, C. Haimbaugh, H. Bichraoui, Y. Du, J.R. Bankston, L.A. Walker, and C. Proenza. 2020. Isoform-specific regulation of HCN4 channels by a family of endoplasmic reticulum proteins. *Proc Natl Acad Sci U S A*. 117:18079–18090. doi:10.1073/pnas.2006238117.

Peters, C.H., D.A. Peraza, L.M. Blecker, J. Bankston, and C. Proenza. 2023. Calcium inhibits the funny current (If)in sinoatrial myocytes. *Biophysical Journal*. 122:380a. doi:10.1016/j.bpj.2022.11.2088.

Peters, C.H., R.K. Singh, J.R. Bankston, and C. Proenza. 2022. Regulation of HCN Channels by Protein Interactions. *Front Physiol*. 13:928507. doi:10.3389/fphys.2022.928507.

Porro, A., A. Saponaro, F. Gasparri, D. Bauer, C. Gross, M. Pisoni, G. Abbandonato, K. Hamacher, B. Santoro, G. Thiel, and A. Moroni. 2019. The HCN domain couples voltage gating and cAMP response in hyperpolarization-activated cyclic nucleotide-gated channels. *eLife*. 8:e49672. doi:10.7554/eLife.49672.

Proenza, C., N. Tran, D. Angoli, K. Zahynacz, P. Balcar, and E.A. Accili. 2002. Different Roles for the Cyclic Nucleotide Binding Domain and Amino Terminus in Assembly and Expression of Hyperpolarization-activated, Cyclic Nucleotide-gated Channels*. *Journal of Biological Chemistry*. 277:29634–29642. doi:10.1074/jbc.M200504200.

Prüschenk, S., M. Majer, R. Schreiber, and J. Schlossmann. 2021. IRAG2 Interacts with IP3-Receptor Types 1, 2, and 3 and Regulates Intracellular Ca2+ in Murine Pancreatic Acinar Cells. *International Journal of Molecular Sciences*. 22:13409. doi:10.3390/ijms222413409.

Santoro, B., L. Hu, H. Liu, A. Saponaro, P. Pian, R.A. Piskorowski, A. Moroni, and S.A. Siegelbaum. 2011. TRIP8b regulates HCN1 channel trafficking and gating through two distinct C-terminal interaction sites. *J. Neurosci.* 31:4074–4086. doi:10.1523/JNEUROSCI.5707-10.2011.

Santoro, B., B.J. Wainger, and S.A. Siegelbaum. 2004. Regulation of HCN Channel Surface Expression by a Novel C-Terminal Protein-Protein Interaction. *J. Neurosci.* 24:10750–10762. doi:10.1523/JNEUROSCI.3300-04.2004.

Saponaro, A., D. Bauer, M.H. Giese, P. Swuec, A. Porro, F. Gasparri, A.S. Sharifzadeh, A. Chaves-Sanjuan, L. Alberio, G. Parisi, G. Cerutti, O.B. Clarke, K. Hamacher, H.M. Colecraft, F. Mancia, W.A. Hendrickson, S.A. Siegelbaum, D. DiFrancesco, M. Bolognesi, G. Thiel, B. Santoro, and A. Moroni. 2021. Gating movements and ion permeation in HCN4 pacemaker channels. *Mol Cell*. 81:2929-2943.e6. doi:10.1016/j.molcel.2021.05.033.

Saponaro, A., F. Cantini, A. Porro, A. Bucchi, D. DiFrancesco, V. Maione, C. Donadoni, B. Introini, P. Mesirca, M.E. Mangoni, G. Thiel, L. Banci, B. Santoro, and A. Moroni. 2018. A synthetic peptide that prevents cAMP regulation in mammalian hyperpolarization-activated cyclic nucleotide-gated (HCN) channels. *eLife*. 7:e35753. doi:10.7554/eLife.35753.

Schlossmann, J., A. Ammendola, K. Ashman, X. Zong, A. Huber, G. Neubauer, G.X. Wang, H.D. Allescher, M. Korth, M. Wilm, F. Hofmann, and P. Ruth. 2000. Regulation of intracellular calcium by a signalling complex of IRAG, IP3 receptor and cGMP kinase Ibeta. *Nature*. 404:197–201. doi:10.1038/35004606.

Shintre*, C., A.C.W. Pike*, A. Tessitore, L. Shrestha, S. Mukhopadhyay, J. Huiskonen, K. Benndorf, J. Kusch, N.A. Burgess-Brown, and E.P. Carpenter. 2018. Human Hyperpolarization Activated Cyclic Nucleotide Gated Ion Channel 4 (HCN4); A Target Enabling Package. doi:10.5281/zenodo.4275875.

Sunkara, M.R., T. Schwabe, G. Ehrlich, J. Kusch, and K. Benndorf. 2018. All four subunits of HCN2 channels contribute to the activation gating in an additive but intricate manner. *J Gen Physiol*. 150:1261–1271. doi:10.1085/jgp.201711935.

Tran, N., C. Proenza, V. Macri, F. Petigara, E. Sloan, S. Samler, and E.A. Accili. 2002. A Conserved Domain in the NH2 Terminus Important for Assembly and Functional Expression of Pacemaker Channels*. *Journal of Biological Chemistry*. 277:43588–43592. doi:10.1074/jbc.M208477200.

Wainger, B.J., M. DeGennaro, B. Santoro, S.A. Siegelbaum, and G.R. Tibbs. 2001. Molecular mechanism of cAMP modulation of HCN pacemaker channels. *Nature*. 411:805–810. doi:10.1038/35081088.

Wang, J.-J., F. Liu, F. Yang, Y.-Z. Wang, X. Qi, Y. Li, Q. Hu, M.X. Zhu, and T.-L. Xu. 2020a. Disruption of auto-inhibition underlies conformational signaling of ASIC1a to induce neuronal necroptosis. *Nat Commun*. 11:475. doi:10.1038/s41467-019-13873-0.

Wang, Z.-J., I. Blanco, S. Hayoz, and T.I. Brelidze. 2020b. The HCN domain is required for HCN channel cell-surface expression and couples voltage- and cAMP-dependent gating mechanisms. *J Biol Chem*. 295:8164–8173. doi:10.1074/jbc.RA120.013281.

Weißgraeber, S., A. Saponaro, G. Thiel, and K. Hamacher. 2017. A reduced mechanical model for cAMP-modulated gating in HCN channels. *Sci Rep*. 7:40168. doi:10.1038/srep40168.

Wicks, N.L., K.S.C. Chan, Z. Madden, B. Santoro, and E.C. Young. 2009. Sensitivity of HCN channel deactivation to cAMP is amplified by an S4 mutation combined with activation mode shift. *Pflugers Arch*. 458:877–889. doi:10.1007/s00424-009-0687-6.

Wicks, N.L., T. Wong, J. Sun, Z. Madden, and E.C. Young. 2011. Cytoplasmic cAMP-sensing domain of hyperpolarization-activated cation (HCN) channels uses two structurally distinct mechanisms to regulate voltage gating. *Proc Natl Acad Sci U S A*. 108:609–614. doi:10.1073/pnas.1012750108.

Wouters, F.S., P.I.H. Bastiaens, K.W.A. Wirtz, and T.M. Jovin. 1998. FRET microscopy demonstrates molecular association of non-specific lipid transfer protein (nsL-TP) with fatty acid oxidation enzymes in peroxisomes. *The EMBO Journal*. 17:7179–7189. doi:10.1093/emboj/17.24.7179.

Zolles, G., D. Wenzel, W. Bildl, U. Schulte, A. Hofmann, C.S. Müller, J.-O. Thumfart, A. Vlachos, T. Deller, A. Pfeifer, B.K. Fleischmann, J. Roeper, B. Fakler, and N. Klöcker. 2009. Association with the auxiliary subunit PEX5R/Trip8b controls responsiveness of HCN channels to cAMP and adrenergic stimulation. *Neuron*. 62:814–825. doi:10.1016/j.neuron.2009.05.008.

Zong, X., S. Krause, C.-C. Chen, J. Krüger, C. Gruner, X. Cao-Ehlker, S. Fenske, C. Wahl-Schott, and M. Biel. 2012. Regulation of Hyperpolarization-activated Cyclic Nucleotide-gated (HCN) Channel Activity by cCMP. *J. Biol. Chem.* 287:26506–26512. doi:10.1074/jbc.M112.357129.

Table 1: Midpoints of Activation for HCN Channel Constructs

	Control	+LRMP	LRMP vs. Control
HCN4	-117.8 ± 0.9 (54)	-120.1 ± 2.2 (14)	P = 0.3530
+cAMP	-103.4 ± 1.5 (36)	-114.7 ± 2.6 (16)	**P < 0.0001**
	P < 0.0001	P = 0.0724	
HCN2	-109.3 ± 1.5 (8)	-114.4 ± 1.9 (8)	P = 0.1101
+cAMP	-90.3 ± 3.2 (8)	-87.9 ± 1.6 (8)	P = 0.4293
	P < 0.0001	**P < 0.0001**	
HCN4 Δ1-25	-118.1 ± 2.2 (19)	-121.0 ± 2.7 (10)	P = 0.3859
+cAMP	-101.1 ± 2.6 (13)	-116.5 ± 1.5 (12)	**P = 0.0001**
	P < 0.0001	P = 0.2236	
HCN4 Δ1-62	-116.5 ± 1.7 (8)	-118.8 ± 1.9 (10)	P = 0.4089
+cAMP	-99.1 ± 2.2 (10)	-107.9 ± 1.4 (8)	**P = 0.0027**
	P < 0.0001	**P = 0.0003**	
HCN4 Δ1-130	-115.2 ± 2.2 (11)	-117.4 ± 1.3 (6)	P = 0.5651
+cAMP	-101.3 ± 2.3 (8)	-106.9 ± 3.7 (7)	P = 0.1481
	P = 0.0003	**P = 0.0152**	
HCN4 Δ1-185	-117.1 ± 2.1 (12)	-125.5 ± 2.3 (8)	P = 0.0500
+cAMP	-103.1 ± 3.3 (13)	-103.6 ± 3.1 (8)	P = 0.8913
	P < 0.0001	**P < 0.0001**	
HCN4 V604X	-101.7 ± 2.0 (12)	-102.0 ± 1.9 (6)	P = 0.9407
+cAMP	-104.7 ± 4.9 (6)	—	—
	P = 0.4698		
HCN4 S719X	-124.9 ± 1.3 (17)	-121.4 ± 1.6 (20)	P = 0.1217
+cAMP	-106.5 ± 1.6 (22)	-114.1 ± 1.6 (18)	**P = 0.0010**
	P < 0.0001	**P = 0.0018**	
HCN4 PT/AF	-127.6 ± 1.6 (21)	-127.8 ± 1.9 (15)	P = 0.9311
+cAMP	-117.1 ± 2.2 (15)	-112.1 ± 2.1 (15)	P = 0.0785
	P = 0.0002	**P < 0.0001**	
HCN2 AF/PT	-106.5 ± 1.9 (15)	-107.7 ± 1.5 (11)	P = 0.5858
+cAMP	-88.2 ± 0.7 (16)	-86.4 ± 1.6 (13)	P = 0.3987
	P < 0.0001	**P < 0.0001**	
HCN4-2	-114.6 ± 2.5 (14)	-111.8 ± 2.0 (15)	P = 0.4270
+cAMP	-94.7 ± 2.9 (16)	-102.5 ± 1.8 (17)	**P = 0.0182**
	P < 0.0001	**P = 0.0059**	
HCN4-2 VVGPT	-104.6 ± 2.1 (16)	-100.9 ± 2.3 (14)	P = 0.2183
+cAMP	-89.6 ± 2.3 (16)	-99.9 ± 1.2 (11)	**P = 0.0019**
	P < 0.0001	P = 0.7574	

Average midpoint of activation ± standard error of the mean (Number of independent cells)

Table 2: Midpoints of Activation in HCN4 in the Presence of LRMP Fragments

	Control	**cAMP (1mM)**	**P-Value Control vs. cAMP**
HCN4 Control	-117.8 ± 0.9 (54)	-103.4 ± 1.5 (36)	**P < 0.0001**
HCN4 LRMP 1-479Cit	-119.8 ± 2.0 (12) P = 0.4077	-117.1 ± 2.2 (11) **P < 0.0001**	P = 0.3941
HCN4 LRMP 1-227	-117.9 ± 1.9 (13) P = 0.9427	-118.1 ± 1.4 (11) **P < 0.0001**	P = 0.9659
HCN4 LRMP 228-539	-116.1 ± 2.6 (9) P = 0.5463	-106.2 ± 3.8 (10) P = 0.3118	**P = 0.0058**
HCN4 LRMP 1-108	-123.1 ± 1.8 (7) P = 0.0894	-103.0 ± 2.5 (8) P = 0.8943	**P < 0.0001**
HCN4 LRMP 110-230	-118.0 ± 4.0 (9) P = 0.945	-106.4 ± 1.3 (12) P = 0.2342	**P = 0.0009**

Average midpoint of activation ± standard error of the mean (Number of independent cells)

Table 3: Acceptor Photobleaching FRET Between LRMP and HCN Channel Fragments

Citrine	Cerulean	FRET Efficiency (%)	P-Value vs. Control
Citrine	HCN4 1-125 or 125-260	1.7 ± 0.3	
	HCN4 1-125	1.6 ± 0.6 (5)	
	HCN4 125-260	1.8 ± 0.4 (11)	
LRMP 1-230	HCN4 1-260	3.6 ± 0.9 (12)	P = 0.8471
	HCN4 1-125	13.1 ± 1.9 (8)	**P < 0.0001**
	HCN4 125-260	14.0 ± 1.9 (4)	**P < 0.0001**
	HCN4 CNBD	0.8 ± 0.5 (5)	P = 1.0000
LRMP 1-108	HCN4 1-260	7.9 ± 1.0 (4)	**P = 0.0265**
	HCN4 1-125	10.4 ± 1.1 (7)	**P < 0.0001**
	HCN4 125-260	11.7 ± 1.3 (9)	**P < 0.0001**
	HCN4 CNBD	0.0 ± 0.5 (6)	P = 0.9869
	HCN2 N-Term	2.4 ± 0.8 (9)	P = 1.0000
LRMP 110-230	HCN4 1-125	17.2 ± 2.5 (8)	**P < 0.0001**
	HCN4 125-260	15.0 ± 2.0 (6)	**P < 0.0001**
	HCN4 CNBD	0.3 ± 0.9 (7)	P = 0.9949
	HCN2 N-Term	2.1 ± 0.8 (8)	P = 1.0000

Average midpoint of activation ± standard error of the mean (Number of independent cells)

Table S1: DNA Constructs Used in this Study

Construct	Plasmid	Tag	Source
HCN1	pCDNA3.1	None	Dr. Eric Accili
HCN2	pCDNA3.1	None	
HCN2 A467P/F469T	pTwist-CMV-WPRE-Neo	None	Twist Biosciences
HCN4 Δ1-25	pCDNA6	None	Dr. Richard Aldrich
HCN4 Δ1-62	pTwist-CMV-WPRE-Neo	None	
HCN4 Δ1-130	pTwist-CMV-WPRE-Neo	None	
HCN4 Δ1-185	pTwist-CMV-WPRE-Neo	none	
HCN4 Δ1-200	pTwist-CMV-Hygro	None	Twist Biosciences
HCN4 P545A/T547F	pCDNA3.1	None	ABM
HCN4 V604X	pCDNA3.1	None	ABM
HCN4 S719X	pCDNA3.1	None	
HCN4-2	pCDNA3.1	None	
HCN4-2 VVGPT	pTwist-CMV-BG-WPRE-Neo	None	Twist Biosciences
LRMP	pCMV6 Kan/Neo	None	Origene
Myc-LRMP	pCMV6 Kan/Neo	Myc-Tag	
LRMP 1-227	pTwist-CMV	Myc-Tag	Twist Biosciences
LRMP 228-539	pTwist-CMV	Myc-Tag	Twist Biosciences
HCN4 1to125	pcDNA3.1	C-term Cerulean	
HCN4 125to260	pcDNA3.1	C-term Cerulean	
HCN4 1to260	pcDNA3.1	C-term Cerulean	
HCN4 CNBD (521-719)	pcDNA3.1	C-term Cerulean	
LRMP 1to479	pcMVBG	C-term Citrine	
LRMP 1-230	pcMVBG	C-term Citrine	
LRMP 110to230	pcMVBG	C-term Citrine	
LRMP 1to108	pcMVBG	C-term Citrine	

Figure 1

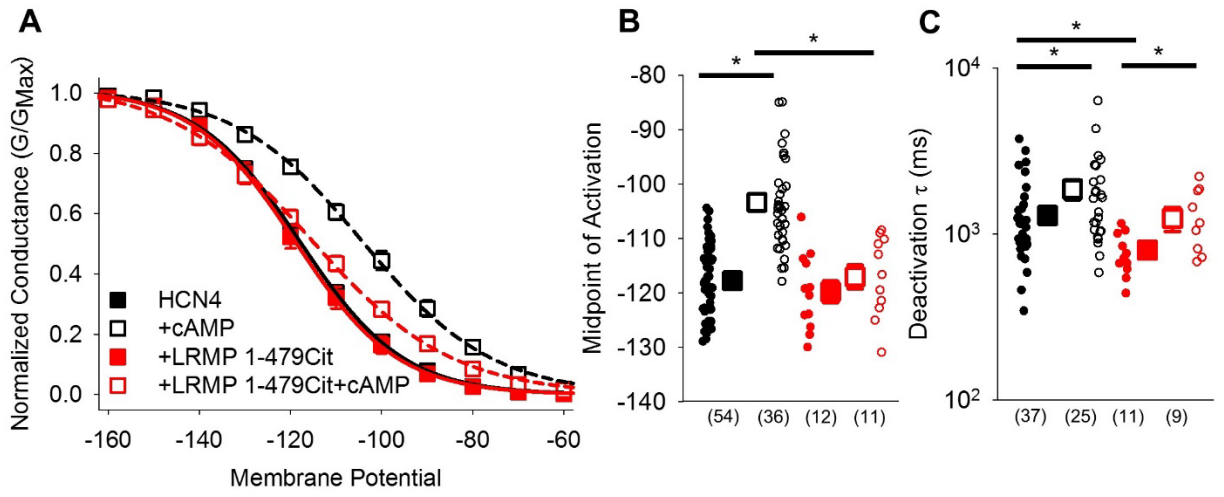

Figure 1: The cytosolic region of LRMP regulates HCN4 but does not antagonize cAMP binding.

A: Voltage dependence of activation for HCN4 alone (*black*) or co-transfected with LRMP 1-479Cit (*red*) in the presence or absence of 1 mM intracellular cAMP (*open symbols*). **B:** Average (± standard error of the mean) midpoints of activation for HCN4 in the absence or presence of LRMP 1-479Cit and/or 1 mM cAMP using the same colour scheme as **A**. **C:** Average (± standard error of the mean) time constants of deactivation for HCN4 in the absence or presence of LRMP 1-479Cit and/or 1mM cAMP using the same colour scheme as **A**. Small circles in **B** and **C** represent individual cells and values in parentheses are the number of independent recordings for each condition. * indicates a significant ($P < 0.05$) difference. All means, standard errors, and exact P-values are in Table 1.

Figure 2

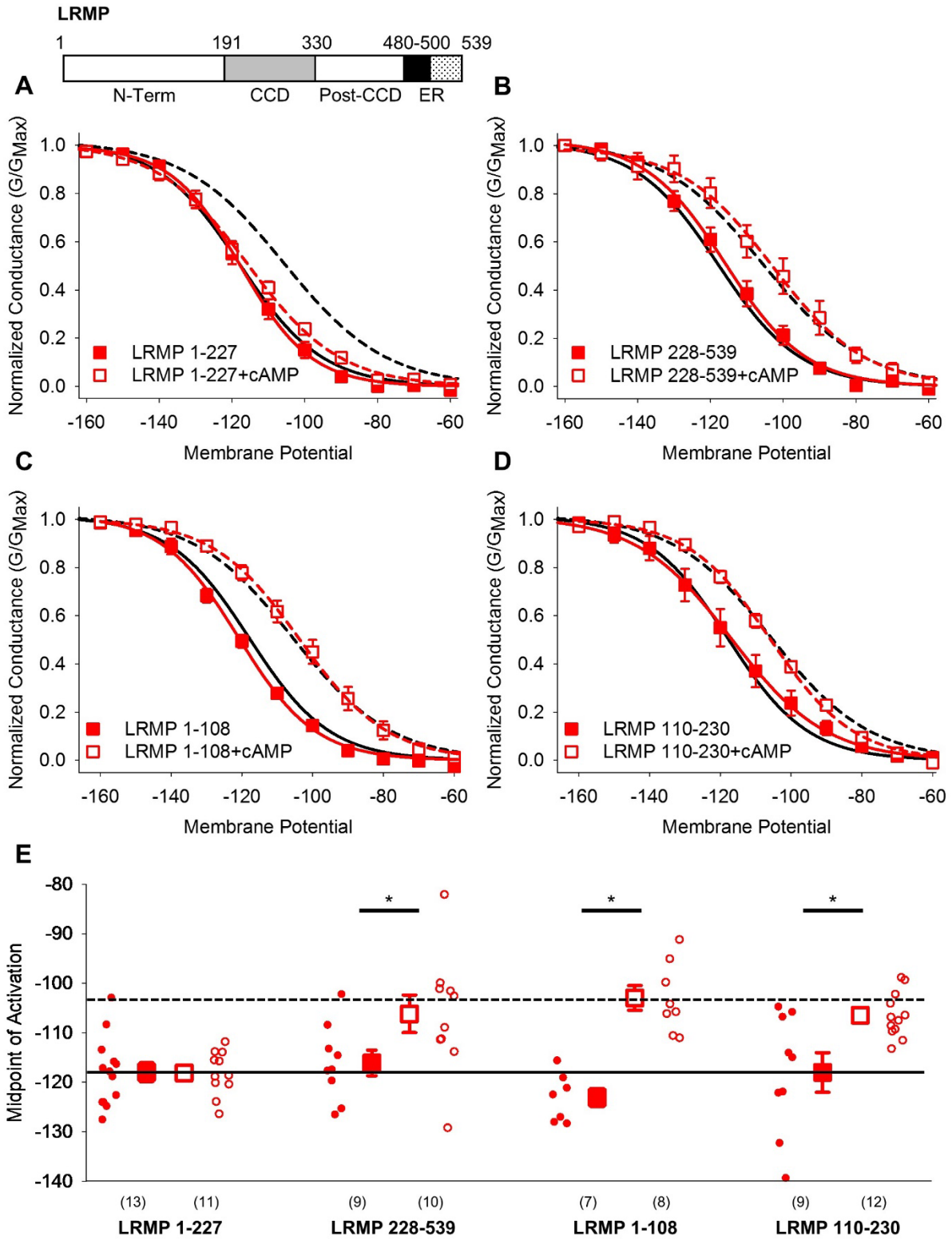
LRMP
1
191
330
480-500
539
N-Term
CCD
Post-CCD
ER
A
B
C
D
E
Normalized Conductance (G/GMax)
Membrane Potential
LRMP 1-227
LRMP 1-227+cAMP
LRMP 228-539
LRMP 228-539+cAMP
LRMP 1-108
LRMP 1-108+cAMP
LRMP 110-230
LRMP 110-230+cAMP
Midpoint of Activation
(13)
(11)
(9)
(10)
(7)
(8)
(9)
(12)
LRMP 1-227
LRMP 228-539
LRMP 1-108
LRMP 110-230

Figure 2: The pre-coiled-coil region of the LRMP N-terminus is necessary and sufficient to regulate HCN4.

A-D: Voltage-dependence of activation for HCN4 in the absence (*black*) or presence (*red*) of LRMP 1-227 (**A**), LRMP 228-539 (**B**), LRMP 1-108 (**C**), or LRMP 110-230 (**D**), and/or 1mM intracellular cAMP (*open symbols*). The midpoints of activation for HCN4 with (*dotted line*) or without (*solid line*) 1 mM cAMP in the absence of LRMP are shown. **A *inset*:** Schematic of LRMP showing the predicted coiled-coil domain (CCD) and ER-transmembrane and luminal domains (ER). **E:** Average (± standard error of the mean) midpoints of activation for HCN4 in the absence or presence of LRMP constructs and/or 1mM cAMP using the same colour scheme as **A-D**. Small circles represent individual recordings and values in parentheses are the number of independent recordings for each condition. * indicates a significant ($P < 0.05$) difference. All means, standard errors, and exact P-values are in Table 2.

Figure 3

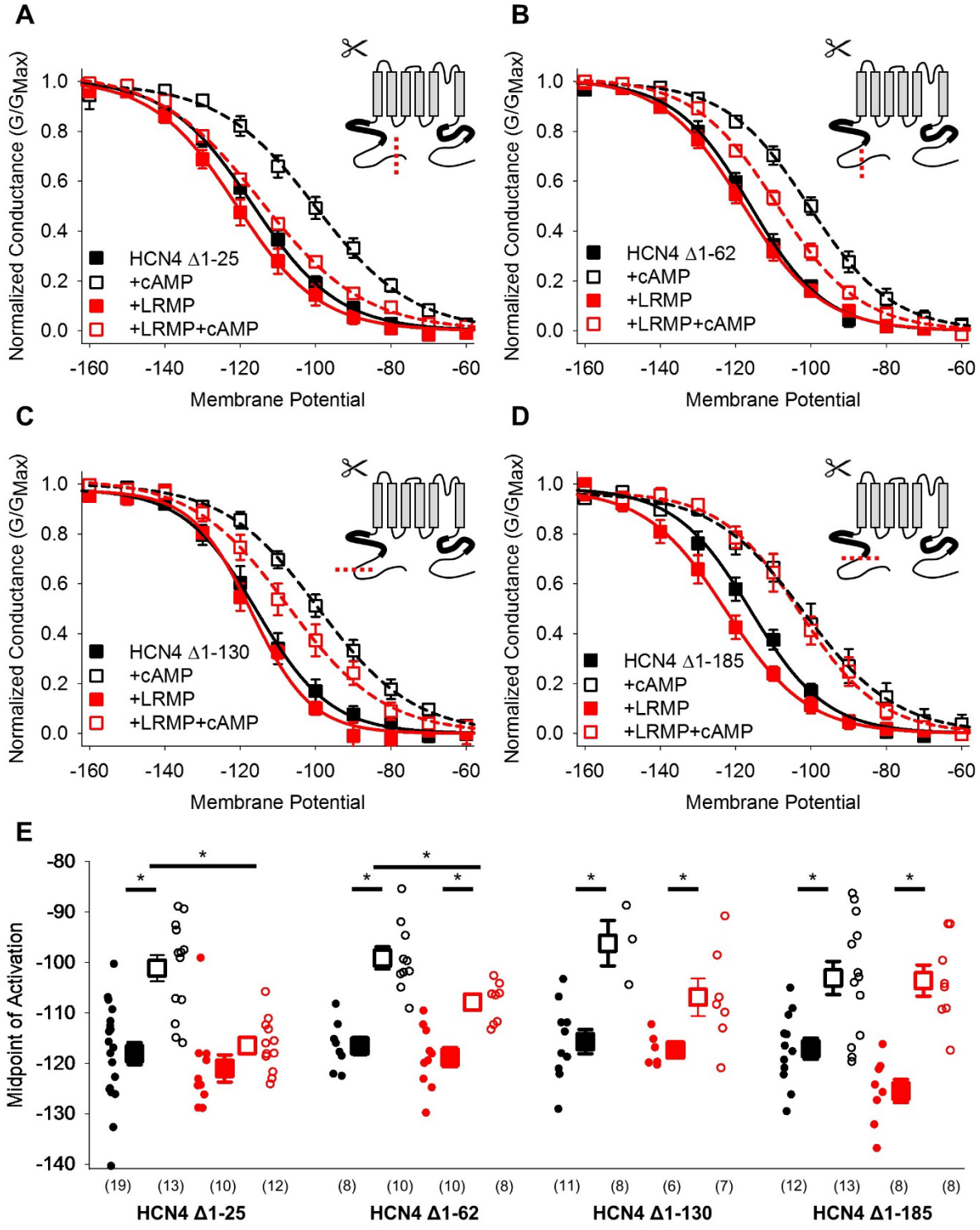

Figure 3: The distal HCN4 N-terminus is required for functional regulation by LRMP.

A-D: Voltage-dependence of activation for HCN4 Δ1-25 (**A**), HCN4 Δ1-62 (**B**), HCN4 Δ1-130 (**C**), and HCN4 Δ1-185 (**D**) in the absence (*black*) or presence of LRMP (*red*) and/or 1mM intracellular cAMP (*open symbols*). **E:** Average (± standard error of the mean) midpoints of activation for HCN4 Δ1-25, HCN4 Δ1-62, HCN4 Δ1-130, and HCN4 Δ1-185 in the absence or presence of LRMP and/or 1mM cAMP using the same colour scheme as **A**. Small circles represent individual recordings and values in parentheses are the number of independent recordings for each condition. * indicates a significant ($P < 0.05$) difference. All means, standard errors, and exact P-values are in Table 1.

Figure 4

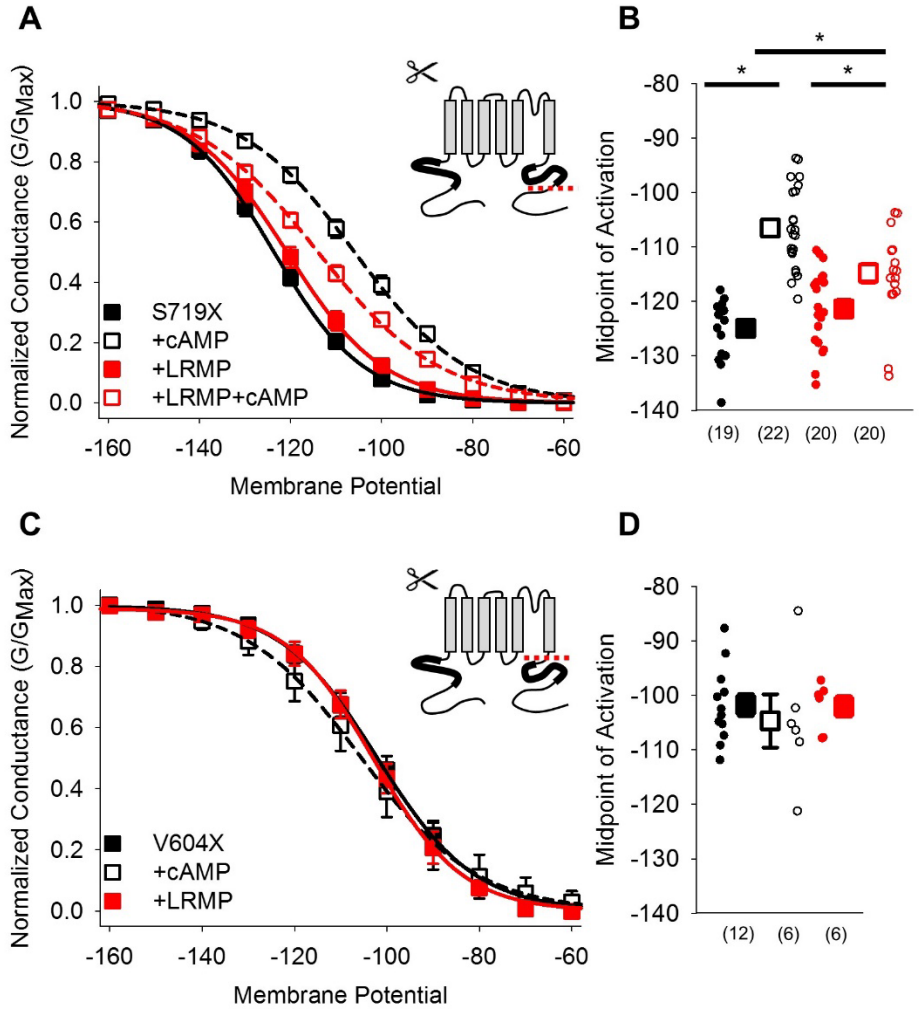

Figure 4: The HCN4 C-terminus is not the primary site for functional regulation by LRMP.

A: Voltage-dependence of activation for HCN4 S719X in the absence (*black*) or presence of LRMP (*red*) and/or 1mM intracellular cAMP (*open symbols*). **B:** Average (± standard error of the mean) midpoints of activation for HCN4 S719X in the absence or presence of LRMP and/or 1mM cAMP using the same colour scheme as **B**. **C:** Voltage-dependence of activation for HCN4 V604X in the absence or presence of LRMP or 1mM intracellular cAMP using the same colour scheme as **B**. **D:** Average (± standard error of the mean) midpoints of activation for HCN4

V604X in the absence or presence of LRMP or 1mM cAMP using the same colour scheme as **B**. Small circles represent individual recordings in **B** and **D** and values in parentheses are the number of independent recordings for each condition. * indicates a significant ($P < 0.05$) difference. All means, standard errors, and exact P-values are in Tables 1 and 3.

Figure 5

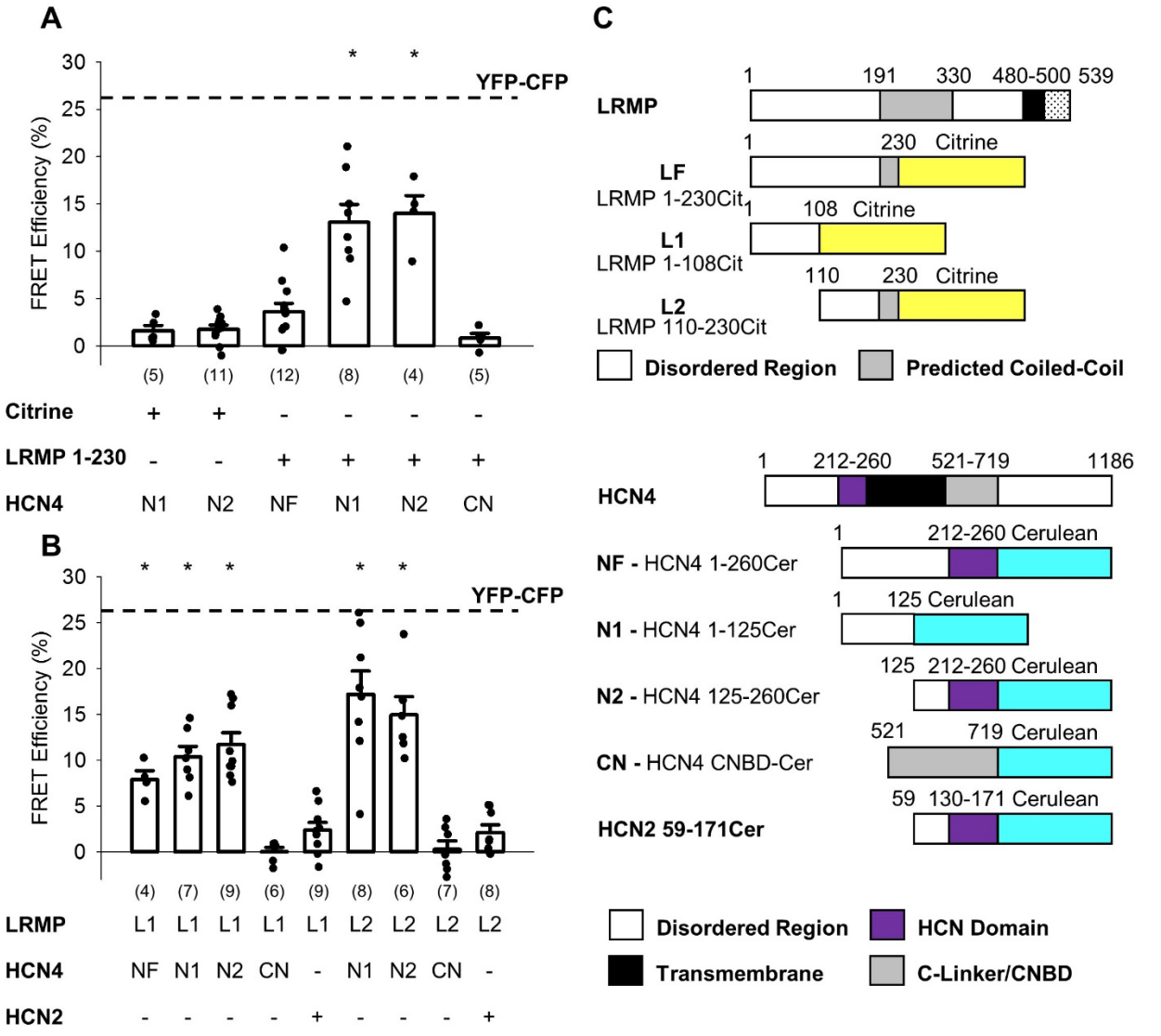

Figure 5: The N-terminus of LRMP FRETs with the N-terminus of HCN4

A: Average (± standard error of the mean) acceptor photobleaching FRET efficiency between Citrine or the Citrine-tagged N-terminal region of the LRMP and Cerulean-tagged fragments of HCN4. The dotted line is the average FRET in YFP-CFP concatemers from a prior study (Wang et al., 2020a). **B:** Average (± standard error of the mean) acceptor photobleaching FRET efficiency between Citrine-tagged fragments of the LRMP N-terminus and Cerulean-tagged fragments of HCN4 or HCN2. Small circles in **A** and **B** represent individual recordings and

values in parentheses are the number of independent recordings for each condition. * indicates a significant ($P < 0.05$) difference compared to control FRET in cells co-transfected with Citrine and with Cerulean-tagged HCN4 N-terminal fragments. All means, standard errors, and exact P-values are in Table 3. **C:** Schematic representations of the Citrine-tagged LRMP fragments and Cerulean-tagged HCN4 and HCN2 fragments used in FRET experiments.

Figure 6

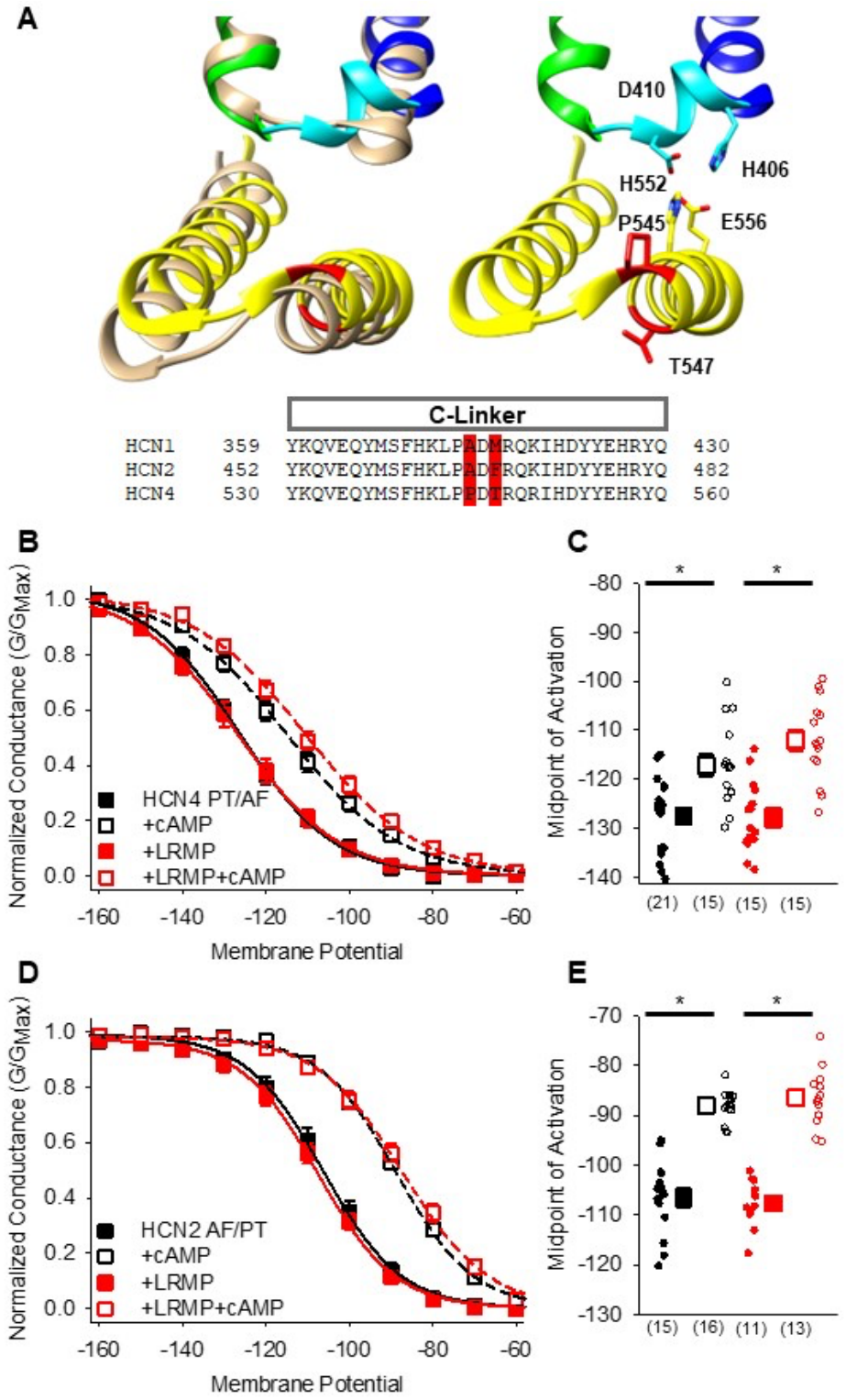

Figure 6: Mutants in the HCN4 C-linker disrupt LRMP's functional effects.

A: Structure of the HCN4 C-linker (PDB: 7NP4) and S4-S5 linker overlapped with HCN1 (PDB: 5U6P; *beige*; *top left*) or showing key residues (*top right*). Alignments of the HCN2 and HCN4 C-linker sequences with the HCN4 P545/T547 sites highlighted in red (*bottom*). **B:** Voltage-dependence of activation for HCN4 P545A/T547F (PT/AF) in the absence (*black*) or presence of LRMP (*red*) and/or 1mM intracellular cAMP (*open symbols*). **C:** Average (± standard error of the mean) midpoints of activation for HCN4 PT/AF in the absence or presence of LRMP and/or 1mM cAMP using the same colour scheme as **B**. **D:** Voltage-dependence of activation for HCN2 A467P/F469T (AF/PT) in the absence or presence of LRMP and/or 1mM intracellular cAMP using the same colour scheme as **B**. **E:** Average (± standard error of the mean) midpoints of activation for HCN2 AF/PT in the absence or presence of LRMP and/or 1mM cAMP using the same colour scheme as **B**. Small circles represent individual recordings in **C** and **E** and values in parentheses are the number of independent recordings for each condition. * indicates a significant ($P < 0.05$) difference. All means, standard errors, and exact P-values are in Table 1.

Figure 7

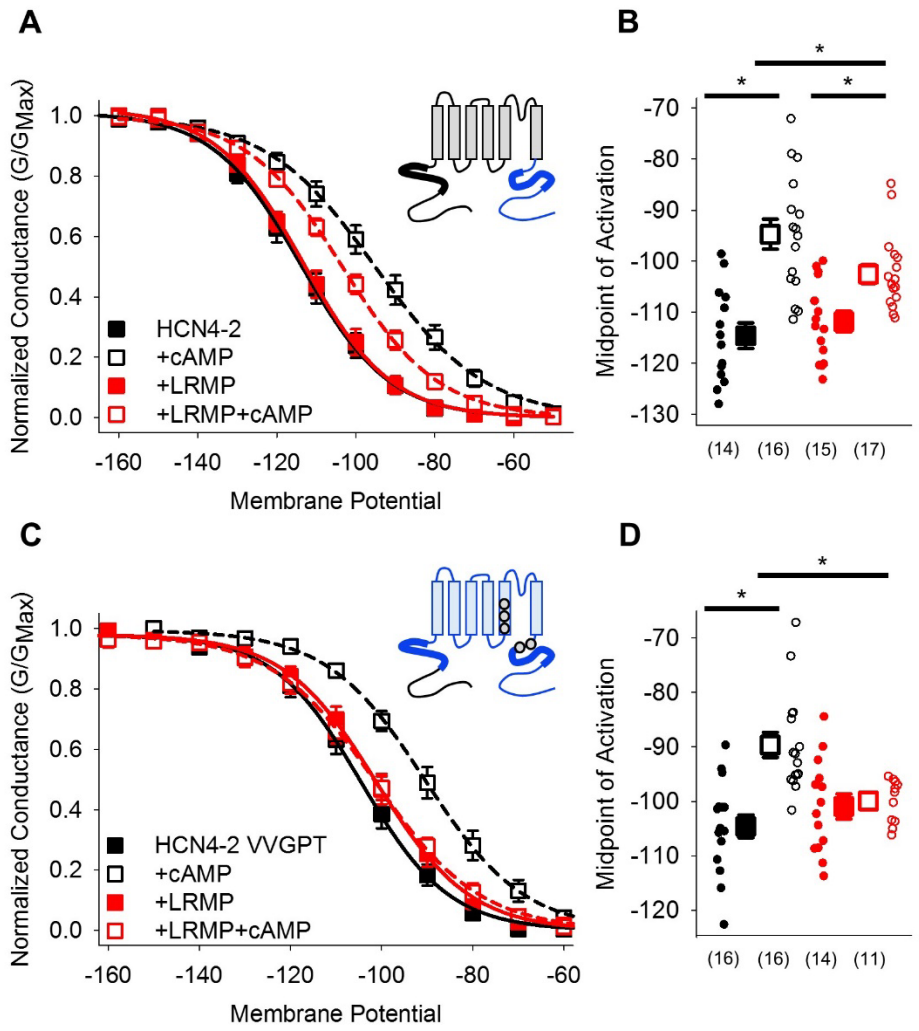

Figure 7: The HCN4 N-terminus confers LRMP regulation on HCN2

A: Voltage-dependence of activation for HCN4-2 (HCN4 1-518 + HCN2 442-863) in the absence (*black*) or presence of LRMP (*red*) and/or 1mM intracellular cAMP (*open symbols*). **B:** Average (± standard error of the mean) midpoints of activation for HCN4-2 in the absence or presence of LRMP and/or 1mM cAMP using the same colour scheme as **A**. **C:** Voltage-dependence of activation for HCN4-2 VVGPT (HCN4 1-212 + HCN2 135-863 M338V/C341V/S345G/A467P/F469T) in the absence or presence of LRMP and/or 1mM intracellular cAMP using the same colour scheme as **A**. **D:** Average (± standard error of the

mean) midpoints of activation for HCN4-2 VVGPT in the absence or presence of LRMP and/or 1mM cAMP using the same colour scheme as **A**. ***Insets*:** Schematics of the HCN4-2 (**A**) and HCN4-2 VVGPT (**C**) channels with HCN4 sequence shown in black and HCN2 in blue. Small circles represent individual recordings in **B** and **D** and values in parentheses are the number of independent recordings for each condition. * indicates a significant ($P < 0.05$) difference. All means, standard errors, and exact P-values are in Table 1.

Figure 8

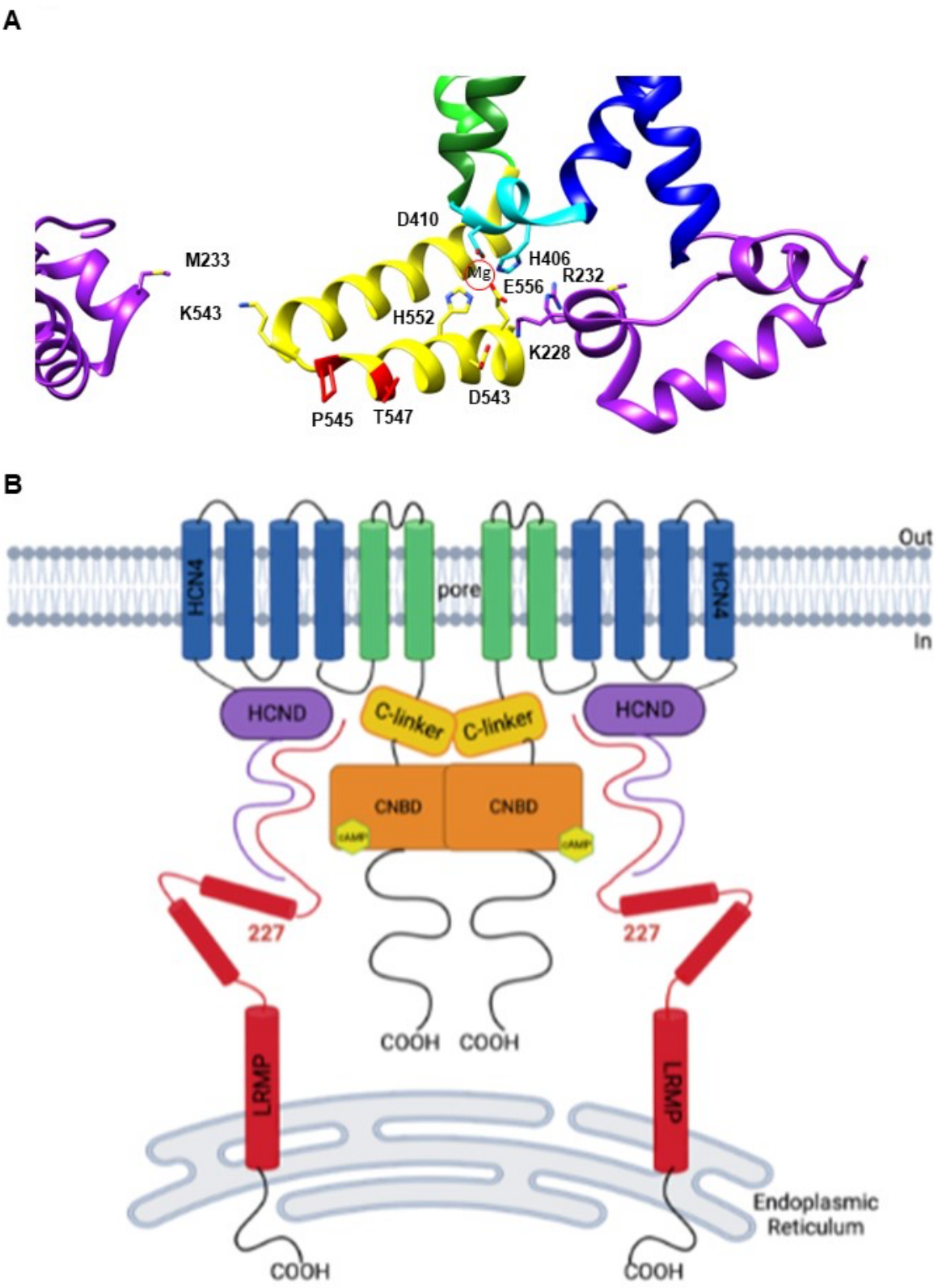
A
D410
M233
H406
Mg
R232
E556
K543
H552
K228
D543
P545
T547
B
Out
In
HCN4
pore
HCN4
HCND
C-linker
C-linker
HCND
CNBD
CNBD
227
227
COOH
COOH
LRMP
LRMP
Endoplasmic
Reticulum
COOH
COOH

Figure 8: Model of interactions between HCN4 and LRMP

A: Structure of the cAMP-transduction centre in HCN4 formed by the C-linker (*yellow*), S4-S5 linker (*teal*), and HCNDs of two subunits (*purple*; PDB: 7NP4). **B:** Schematic of the proposed interactions between LRMP (*red*) and the HCN4 channel. The cytoplasmic N-terminus of LRMP interacts with the HCN4 N-terminus to functionally regulate cAMP-dependent shifts in activation at the interface between the N-terminus, C-linker, and S4-S5 linker. Made with BioRender.